ELSEVIER

Contents lists available at ScienceDirect

Developmental Biology

journal homepage: www.elsevier.com/locate/developmentalbiology



Diacylglycerol, PKC and MAPK signaling initiate tubeworm metamorphosis in response to bacteria



Kyle E. Malter ^{a,b}, Milagros Esmerode ^{a,b}, Myedith Damba ^{b,c}, Amanda T. Alker ^{a,b}, Erica M. Forsberg ^{b,c}, Nicholas J. Shikuma ^{a,b,*}

- ^a Department of Biology, San Diego State University, San Diego, CA, 92182, USA
- ^b Viral Information Institute, San Diego State University, San Diego, CA, 92182, USA
- ^c Department of Chemistry and Biochemistry, San Diego State University, San Diego, CA, 92182, USA

ABSTRACT

External environmental cues can have significant impacts on the timing and outcomes of animal development. For the swimming larvae of many marine invertebrates, the presence of specific surface-bound bacteria are important cues that help larvae identify a suitable location on the sea floor for metamorphosis and adult life. While metamorphosis in response to bacteria occurs in diverse animals from across the animal tree of life, we know little about the signal transduction cascades stimulated at the onset of metamorphosis upon their interaction with bacteria. The metamorphosis of a model tubeworm, *Hydroides elegans*, is triggered by the bacterium *Pseudoalteromonas luteoviolacea* which produces a stimulatory protein called Mif1. In this work, we define three key nodes in a signaling cascade promoting *Hydroides* metamorphosis in response to Mif1. Using metabolomic profiling, we find that the stimulation of *Hydroides* larvae by *P. luteoviolacea* leads to an increase in diacylglycerol during the initiation of metamorphosis, and that Mif1 is necessary for this upregulation. Genomic and pharmacological examination suggests that diacylglycerol triggers a phosphotransferase signaling cascade involving Protein Kinase C (PKC) and Mitogen-Activated Protein Kinase (MAPK), to induce *Hydroides* metamorphosis. Additionally, Mif1 activates the expression of two nuclear hormone receptors, HeNHR1 and HeNHR2 in the cerebral ganglia of *Hydroides* larvae. Our results define a post-translational signal transduction pathway mediating bacteria-stimulated metamorphosis in a model invertebrate animal.

1. Introduction

How a single-celled zygote develops into a multicellular organism has fascinated scientists for centuries. While animal development was once thought to occur in isolation of the environment, it is now becoming clear that an animal's environmental context can dictate when, where, and how an animal develops (Gilbert et al., 2015). A striking example of this phenomenon is the induction of animal metamorphosis by bacteria (Cavalcanti et al., 2020; Hadfield, 2011), wherein the free-swimming larvae of many bottom-dwelling marine invertebrates use environmental bacteria as an indicator of a preferable habitat before attaching to the sea floor and undergoing metamorphosis (Hadfield et al., 2001). Although the induction of metamorphosis by bacteria was first described in the 1930s (Zobell and Allen, 1934), it remains unclear how animal larvae sense and respond to bacterial cues to undergo this essential life history transition.

Metamorphosis has been studied in detail in amphibians and insects, where internal hormonal cues signal through nuclear hormone receptor (NHR) transcription factors to orchestrate a prolonged, stage-specific, developmental program based on a cascade of gene expression (Brown

and Cai, 2007; Hill et al., 2013; Lawrence et al., 1996; Tata, 1998). In contrast, the free-swimming larvae of many bottom-dwelling marine animals reach a metamorphic competence stage, where they possess the developmental ability to undergo a rapid metamorphosis in response to external cues (Hadfield et al., 2001). This rapid metamorphic transition in response to external cues is thought to help the swimming animal larvae identify a suitable location on the sea floor and transition quickly for survival, growth and reproduction as a juvenile and adult (Hadfield, 2000).

Evidence suggests that the rapid metamorphic response of marine animal larvae is initiated through post-translational signaling mechanisms. In the tubeworm *Hydroides elegans* and the Bryozoan *Bugula neritina*, metamorphosis can begin even in the presence of transcription and translation inhibitors (Carpizo-ituarte and Hadfield, 2003; Thiyagarajan et al., 2009). Comparative proteomics in *B. neritina* during metamorphosis identified a downregulation of two phosphorylated proteins: the mitochondrial processing peptidase beta subunit, and the calcium-dependent actin binding protein Severin, which suggests a role for protein phosphorylation and not *de novo* protein synthesis during metamorphosis initiation (Wong et al., 2010). These studies suggest that

^{*} Corresponding author. Department of Biology, San Diego State University, San Diego, CA, 92182, USA. *E-mail address:* nshikuma@sdsu.edu (N.J. Shikuma).

the machinery required for the initiation of metamorphosis is present once the larvae reach competency.

A number of conserved post-translational signaling systems have been shown to be involved in orchestrating metamorphosis in marine invertebrates. These systems include the cyclic adenosine monophosphate (cAMP) second messengers (Bryan et al., 1997; Liang et al., 2018; Strader et al., 2018), the neurotransmitters serotonin and nitric oxide (NO) (Leise et al., 2001; Li, 2011), alterations in membrane potential (Biggers and Laufer, 1999; Carpizo-Ituarte and Hadfield, 1998; Leitz and Klingmann, 1990; Pearce and Scheibling, 1994; Yool et al., 1986), Mitogen Activated Protein Kinase (MAPK) signaling (Chambon et al., 2007; Shikuma et al., 2016), and the Protein Kinase C (PKC) signaling pathway (Amador-Cano et al., 2006; Biggers and Laufer, 1999; Henningi et al., 1998; Leitz and Klingmann, 1990; Yamamoto et al., 1995). The PKC pathway has been identified within representatives of many major animal phyla, including Hyractinia echinata, Mitrocomella polydiademata and Red Sea coral planulae (Cnidaria), Capitella sp. 1 (Annelida), the barnacle Balanus Amphitrite (Arthropoda) and the sea urchin Strongylocentrotus purpuratus (Echinodermata) (Amador-Cano et al., 2006; Biggers and Laufer, 1999; Freeman and Ridgway, 1990; Henningi et al., 1998; Leitz and Klingmann, 1990; Yamamoto et al., 1995). Of the above-mentioned signaling systems, PKC was activated in response to bacteria in the hydrozoans Hydractinia echinata and Phialidium gregarium (McCauley, 1997; Schneider and Leitz, 1994), while serotonin, membrane potential and MAPK have been implicated in mediating metamorphosis in response to bacteria in the annelid, Hydroides elegans (Carpizo-Ituarte and Hadfield, 1998; Nedved, 2010; Shikuma et al., 2016).

To investigate the animal signaling systems mediating metamorphosis in response to bacteria, we study the metamorphosis of the marine biofouling tubeworm Hydroides elegans (hereafter, Hydroides) (Nedved and Hadfield, 2009). Hydroides was shown previously to undergo metamorphosis in response to a marine bacterium Pseudoalteromonas luteoviolacea, providing a model system to better understand the modes by which bacteria promote animal development (Huang and Hadfield, 2003; Huang et al., 2012; Shikuma, 2021). To induce Hydroides metamorphosis, P. luteoviolacea produces an array of bacteriophage tail-like particles called Metamorphosis Associated Contractile structures (MACs) that are necessary for the bacterium to stimulate metamorphosis (Shikuma et al., 2014, 2016). MACs carry a protein effector called Metamorphosis inducing factor 1 (Mif1) that is required for MACs to induce Hydroides metamorphosis (Ericson et al., 2019). Upon stimulation by MACs, we found previously that the inhibition of either the p38 Mitogen Activated Protein Kinase (p38 MAPK) or c-Jun N-terminal Kinase (JNK) MAPK pathways are critical for Hydroides metamorphosis (Shikuma et al., 2016). However, the other signal transduction events that occur upon the stimulation of Hydroides metamorphosis by MACs and the effector Mif1 remain mysterious.

In this study, we hypothesized that post-translational signal transduction contributes to the orchestration of metamorphosis of *Hydroides* in response to the bacterial protein Mif1. We therefore leverage comparative metabolomics to identify metabolites that are differentially produced during bacteria-stimulated metamorphosis. Our approach utilized mutants of *P. luteoviolacea* that lack an essential component of MACs or the effector Mif1 to identify changes in lipid second messengers. From these analyses, we demonstrate that MACs and Mif1 stimulate three key nodes of post-translational signaling. Mif1 promotes diacylglycerol (DAG) production in *Hydroides*, and we demonstrate that DAG alone is sufficient to induce metamorphosis. Mif1 promotes PKC and MAPK signaling, which upregulates the production of two nuclear hormone receptor genes.

2. Results and discussion

P. luteoviolacea Mif1 promotes broad changes in the lipid profile of tubeworm larvae, including the production of diacylglycerol. To identify the signaling pathways in *Hydroides* that are initiated by MACs

and Mif1, tubeworm larvae were exposed to MACs extracts from P. luteoviolacea wild type or mutants for 1 h to induce a response, as observed previously (Shikuma et al., 2014). We employed a previously developed protocol to isolate MACs from P. luteoviolacea cells, which has been shown to strongly induce Hydroides metamorphosis (Ericson et al., 2019; Shikuma et al., 2014). Larvae were then subjected to total lipid extraction; samples were analyzed by high performance reverse phase liquid chromatography-quadrupole time of flight mass spectrometry (LC-QTOF-MS) and data were analyzed by comparative metabolomics using XCMS (Fig. 1A). To determine the effect of MACs and Mif1 on the Hydroides larvae, we compared the total lipid profile of Hydroides larvae when exposed to (1) MACs extraction buffer alone, (2) MACs extract from wild type P. luteoviolacea, or MACs extract from two mutant *P. luteoviolacea* strains: (3) a strain $\triangle macB$ that lacks the baseplate gene and does not form functional MACs or (4) a strain $\Delta mif1$ that forms intact MACs but lacks the Mif1 effector required for metamorphosis (Ericson et al., 2019; Shikuma et al., 2014). From these analyses, we identified a total of 7683 unique metabolic features identified by m/z ratio.

When we performed comparative metabolomics in a multiple group comparison of all four treatments, we identified 41 differentially regulated lipid products (plotted based on retention time, intensity and sorted by significance (p-value)). XCMS analysis is a preprocessing method that sorts molecules based on a univariate analysis of variance by one-way ANOVA based on relative intensities to identify differentially regulated metabolites vs the baseline mean, and then sorts them based on p-value (Gowda et al., 2014). Forty one significantly dysregulated lipids (p-value <0.01) were visualized as a cloud plot based on their retention time (relative hydrophobicity), intensity (relative abundance), m/z value (mass to charge ratio) and p-value (significant difference) (Fig. 1B and Table S1). Many significantly dysregulated products were identified as small hydrophobic peptides (e.g. Asp, Ile, Asn, and Pro) with a short retention time, eluting before the more hydrophobic lipid products (Table S1). Additionally, we found compounds which had both m/z and retention times consistent with the general membrane components including phosphatidylcholine (PC), phosphatidyl serine (PS), and phosphatidyl ethanolamine (PE). While PC, PS and PE were identified as dysregulated, these components only increased in the $\Delta mif1$ mutant, perhaps in response to sensing the bacterial products. Although this was intriguing, we did not attribute these changes to the signaling required to induce metamorphosis, as MACs lacking Mif1 ($\Delta mif1$) do not induce metamorphosis (Ericson et al., 2019). We did, however, identify an increase of compounds consistent with the class of lipids phosphatidylcholine (PC) and phosphatidylethanolamine (PE) in the wild type condition. It is unclear whether these lipids play a role in the signaling of metamorphosis induction or are perhaps upregulated to support membrane breakdown and/or restructuring during metamorphosis.

Two species of diacylglycerol (DAG, m/z 654.5051, m/z 639.4936) were identified in the multigroup comparison based on the m/z ratio and a retention time and were of particular interest because of their known role as signaling lipids in eukaryotes (Fig. 1B inset b and 1C). The identified diacylglycerols were upregulated when wild type MACs were added to *Hydroides* larvae and metamorphosis had been initiated compared to treatments where extraction buffer, or MACs from Δ macB or Δ mif1 were added to larvae and they did not undergo metamorphosis.

Diacylglycerols have previously been characterized as signaling lipids and can be found in all eukaryotes. DAG is responsible for recruiting the cysteine rich C1 domain containing proteins to the membrane and can subsequently activate specific enzymatic functions (Nishizuka, 1992). DAG is canonically produced when a phospholipase C type lipase binds to the membrane and cleaves between the phosphate and the headgroup, leaving behind the glycerol backbone with the two acyl chains (Titball, 1993). Consistent with our observation, previous studies in the Cnidarian, *H. echinata*, showed that DAG was sufficient to stimulate metamorphosis (Leitz and Müller, 1987; Nishizuka, 1995). The C1 binding domain was first discovered in PKC isoforms and has since been identified in many other proteins such as Chimerins, DAG kinases, PKD,

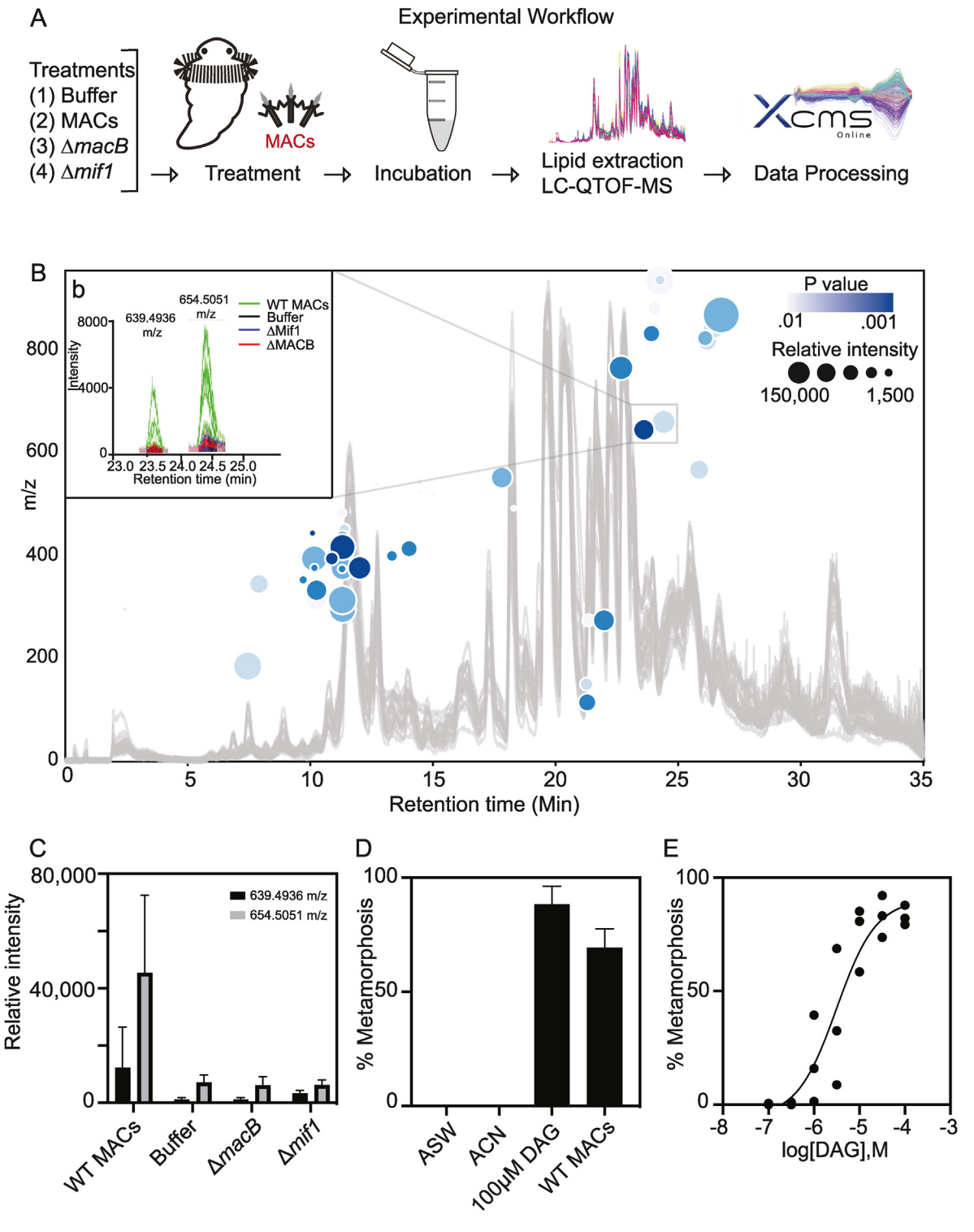


Fig. 1. Lipidomics of *Hydroides elegans* metamorphosis in response to MACs and the role of DAG in metamorphosis initiation. (A) Experimental design showing *Hydroides* larvae treated with extraction buffer, wild type MACs extract, $\Delta macB$ MACs extract or $\Delta mif1$ MACs extract for 1 h before total lipids were removed by chloroform/methanol extraction, lipidomic analyses and data analyses using XCMS. (B) A cloud plot shows all significant features identified by univariate *t*-test (p < 0.01), with more significant features in darker blue and relative intensity indicated by circle size. (b) The inset represents the relative intensity of two DAG molecules across the varying conditions as displayed on the cloud plot. The y-axis represents mass to charge of individually identified compounds, and x-axis represents relative hydrophobicity as the retention time. (C) Relative intensity of signal from two diacylglycerols (m/z = 639.4936) and (m/z = 654.5051) after treatment with extraction buffer, wild type MACs extract, $\Delta macB$ MACs extract or $\Delta mif1$ MACs extract. Metabolomics data are represented as the mean signal intensity \pm SD of n = 6 biological replicates. P-values by one-way ANOVA and Tukey's multiple comparison test between WT MACs and buffer, $\Delta macB$, or $\Delta mif1$ were p-value = 0.0705, 0.0626, and 0.1629 respectively for DAG m/z = 639.4936 and p-value of 0.0006, 0.0004, and 0.0004 for DAG m/z 654.5051. (D) Metamorphosis assay with *Hydroides* larvae in Artificial Seawater (ASW), 1:1,000 acetonitrile solvent control, 100 μ M 1,2-dioctanoyl-sn-glycerol (DAG), or 1:50 dilution of MACs extract. Data are represented as the mean \pm SD of 4 biological replicates. (E) Metamorphosis assay with competent larvae soaked in increasing concentrations of 1,2-dioctanoyl-sn-glycerol (DAG) and assessed for metamorphosis after 24 h 1,2-dioctanoyl-sn-glycerol showed an EC50 of 3.156 \times 10⁻⁶ M. Data show a total of 3 biological replicates (n = 3), where larvae were derived from different male and female individuals; ea

RasGRPs and Munc13s (Brose and Rosenmund, 2002). PKC has been shown to be important for mediating signal transduction during metamorphosis in other marine invertebrates such as *H. echinata* and the Annelid *Capitella* sp. 1 (Biggers and Laufer, 1999; Leitz and Wagner, 1993). Based on our observation that m/z 654.5051 and m/z 639.4936 DAG concentrations were greater in larvae treated with MACs from WT when compared to other treatments and the prior literature connecting DAG with metamorphosis in other animals, we investigated the role of the PKC pathway and its importance for bacteria-stimulated metamorphosis in *Hydroides*.

2.1. The lipid second messenger diacylglycerol stimulates hydroides metamorphosis

To further ascertain the potential role of DAG in the metamorphosis signaling pathway, we tested whether DAG alone is sufficient to induce metamorphosis by exogenously adding 1,2-dioctanoyl-sn-glycerol (a putative PKC activator) to Hydroides larvae. We chose a form of DAG possessing short 8 carbon acyl chains to promote its solubility in seawater. Adding 1,2-dioctanoyl-sn-glycerol to competent Hydroides larvae was sufficient to induce metamorphosis when compared to the solvent controls (Fig. 1D). To determine the sensitivity of larvae to 1,2dioctanoyl-sn-glycerol a dose-response curve showed that Hydroides responds to 1,2-dioctanoyl-sn-glycerol with an EC50 of 3.156 μ M $(\log(3.156 \times 10^{-6}) = -5.501)$ (Fig. 1E). These data show that DAG stimulates metamorphosis in Hydroides at comparable levels to P. luteoviolacea MACs and Mif1. Our results are congruent with previous finding in H. echinata where DAG has been shown to stimulate metamorphosis with similar effective concentrations ranging from 5 µM to 100 µM (Leitz and Müller, 1987).

Hydroides possesses a conserved PKC signaling pathway. DAG signals through several proteins with DAG-binding C1 domains, including PKC. Because PKC signaling has been shown to be important for mediating the metamorphosis in diverse marine animals, we focused

our investigation on the stimulation of PKC by DAG in *Hydroides*. In humans, PKC signaling output is heavily determined by cell type and cell lineage, and different cell types are capable of divergent downstream signaling resultant from the same initial stimulus. There are ten isoforms of PKC in humans (nine not including splice variants), each thought to regulate some distinct, and some overlapping signals (Black and Black, 2012).

To identify PKC isoforms in Hydroides and their expression prior to metamorphosis, we searched the sequenced Hydroides genome (Shikuma et al., 2016) with each of the known human PKC isoforms. Using PSI-BLAST, we identified seven genes encoding proteins with a PKC kinase domain (Fig. 2, Table 1). We used a hidden Markov model domain search (HMMER) to identify the following domains within each putative PKC ortholog; the C2 Ca²⁺ binding domain, the PB1 domain, the C1 DAG/phorbol ester binding domain, a ser/thr protein kinase domain, and the PKC terminal domain (Finn et al., 2011) (Fig. 2, Table S2). A maximum likelihood phylogenetic analysis showed that three Hydroides PKC genes cluster with the Ca²⁺-independent novel human PKC isoforms (Fig. 2). Of the Hydroides genes that cluster with PKC isoforms, XLOC 080992 (hereafter HePKC1) clusters with the novel PKC genes theta and delta isoforms, while XLOC 012419 (hereafter HePKC2) and XLOC 026127/XLOC 043332 (hereafter HePKC3) cluster with the novel PKC genes eta and epsilon isoforms. Four of the Hydroides genes clustered separately from the human PKC isoforms, potentially indicating they are paralogs and may possess an alternative function not relating to PKC. None of the Hydroides genes cluster with the conventional PKC genes and, even though the HePKC1 gene possesses the C2 Ca^{2+} binding domain, the architecture of the gene is more similar to that of the Ca²⁺ independent PKC types theta and delta isoforms. When we searched the Hydroides transcriptome during the competent stage and a timepoint 30-min after the stimulation of metamorphosis by MACs (Shikuma et al., 2016), we found that all isoforms were expressed in the competent larvae (Table 1). Three isoforms increased their expression post induction and four decreased their expression.

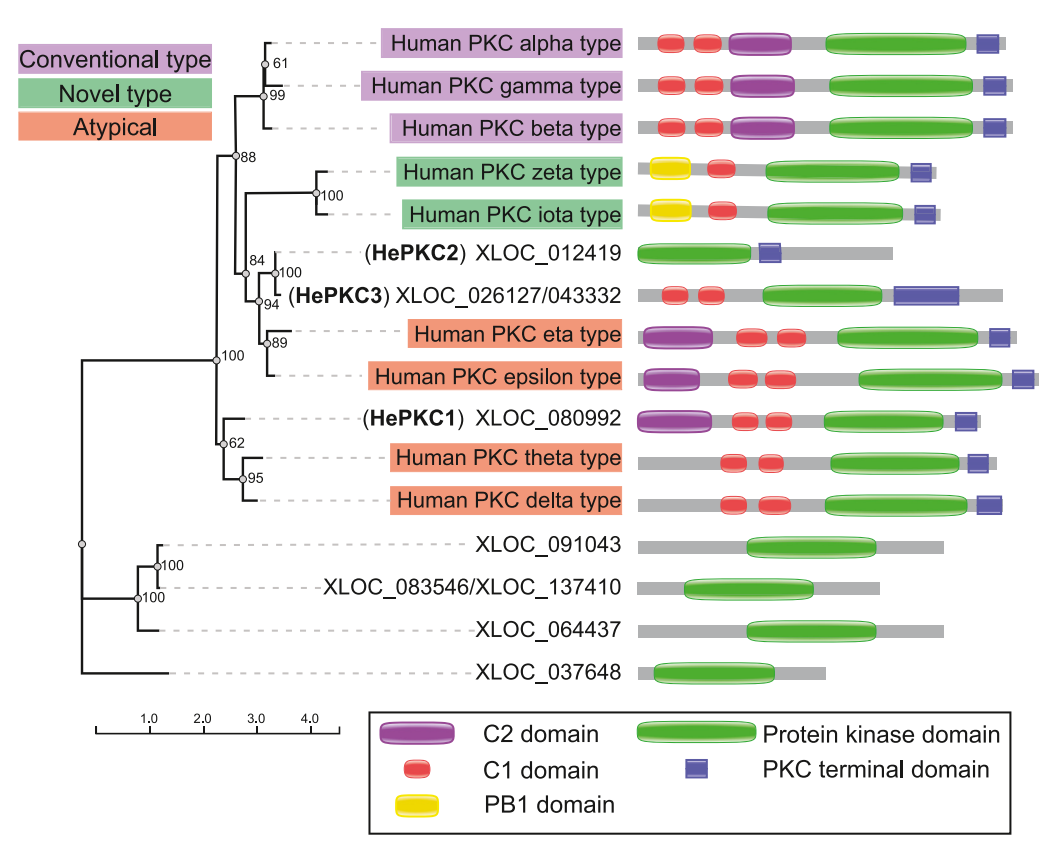


Fig. 2. The Hydroides genome possesses 3 PKC isoforms or homologs. Seven Hydroides PKC isoforms or homologs are represented by a maximum likelihood phylogeny created using a Mafft e-ins-i alignment and PhyML and supported with 100 bootstraps, with nine human PKC isoforms: sp|Q02156| KPCE_HUMAN, sp|Q05513|KPCZ_HU-MAN, sp|P41743|KPCI_HUMAN, sp| P24723 KPCL_HUMAN, sp|P17252| sp|P05129|KPCG_HU-KPCA HUMAN, MAN, sp|P05771|KPCB_HUMAN, sp| Q04759 KPCT_HUMAN, sp|Q05655| KPCD HUMAN. The human PKC genes are color coordinated based on class (conventional, novel, or atypical). All PKC-associated protein domains identified by Pfam and/or Gene3d are displayed beside each branch and color coordinated with accordance to the legend. Three Hydroides homologs cluster with human PKC isoforms: HePKC1, HePKC2 and HePKC3.

Table 1

Homology and expression of *Hydroides PKC* and NHR proteins. Genes identified as PKC or NHR gene isoforms or homologs were identified using PSI-BLAST to identify the closest human or animal homolog or until convergence in which case the top hit is represented. RNA seq Fragments Per Kilobase of transcript per Million mapped reads (FPKM) was identified for larvae at competency (6 days post fertilization) or larvae 30 min post-induction of metamorphosis with *P. luteoviolacea* from previously published data (Shikuma et al., 2016).

Gene ID	Psi-blast Gene Identification	Species Name	Query cover	E-value	% Identity	Competent larvae FPKM	30 min Post- Induction FPKM
XLOC_080992 HePKC1	Protein Kinase C delta a isoform X2	Megalops cyprinoides	99%	0	51.65%	1.37262	1.51084
XLOC_012419	Protein Kinase C epsilon type	Homo sapiens	56%	0	77.22%	1.20571	1.12477
HePKC2							
XLOC_026127/	Protein Kinase C epsilon type	Homo sapiens	74%	0	62.89%	4.17854	4.9028
XLOC_043332							
HePKC3							
XLOC_064437	Protein Kinase C epsilon type	Homo sapiens	73%	0	22.72%	0.0518709	0.0313017
XLOC_091043	Protein Kinase C delta-type	Homo sapiens	77%	0	23.81%	2.04218	1.6393
XLOC_083546/	Protein Kinase C delta-type	Homo sapiens	53%	2.00E-	33.77%	0.0620922	0.0159114
XLOC_137410				48			
XLOC_037648	Protein Kinase C delta type	Myripristis murdjan	94%	0	27.91%	1.29021	1.43314
XLOC_089429	Ecdysone-induced protein	Photinus pyralis	75%	0	21.63%	5.4852	22.6351
HeNHR1							
XLOC_109682	Peroxisome proliferator-activated	Thunnus maccovii	73%	0	22.83%	4.59586	17.6312
HeNHR2	receptor						

Two PKC inhibitors abrogate Hydroides metamorphosis in response to MACs and Mif1. Classical and novel PKC proteins are in the cell cytosol and recruited to the membrane by the presence of DAG. Once activated, they release their pseudo-substrate, a portion of the protein which blocks the active site, and then phosphorylate downstream signaling molecules via ATP cleavage (Nishizuka, 1995). To test whether PKC is important in bacteria-stimulated metamorphosis, we examined the ability of two PKC inhibitors to block Hydroides metamorphosis in response to P. luteoviolacea MACs and Mif1. The first, Ro 32-0432 is a potent active site competitive inhibitor that is highly selective for PKC type kinases and with low affinity for non-PKC kinases (Wu-Zhang and Newton, 2013). Ro 32-0432 exhibits a IC50 of 9-37 nM and 108 nM for conventional PKCs and PKC epsilon, respectively (Fabre et al., 1993; Wilkinson et al., 1993). Although less potent, the second inhibitor bisindolylmaleimide IV (Bis IV) is an allosteric uncompetitive inhibitor that shows a high selectivity for PKC over other kinases (IC50 of 0.55 µM) (Davis et al., 1992; Wu-Zhang and Newton, 2013).

To test Ro 32–0432 and Bis IV on PKC in *Hydroides*, we pre-incubated competent larvae with each inhibitor for 60 min and subsequently exposed the larvae to MACs extracts from *P. luteoviolacea*. We found that Ro 32–0432 inhibited metamorphosis in the presence of MACs in a dose-dependent manner with an IC50 of 235 nM (log(2.35 \times 10 $^{-7}$) = -6.627) (Fig. 3A and B) and Bis IV inhibited with an IC50 concentration of 1.259 μ M (log (1.259 \times 10 $^{-6}$) = -5.900) (Fig. 3A and C). We also tested whether each inhibitor blocked metamorphosis in the presence of DAG as the initiator of metamorphosis. We found that both Ro 32–0432 and Bis IV were capable of inhibiting metamorphosis stimulated by either DAG or MACs (Fig. 3A and D). While it is unclear whether Ro 32–0432 and Bis IV PKC inhibitors block metamorphosis strictly by inhibiting PKC activity, our data show that metamorphosis stimulated by either DAG or MACs is blocked by Ro 32–0432 and Bis IV PKC inhibitors.

We cannot rule out the possibility that Ro 32–0432 and/or Bis IV inhibit other proteins or processes besides the PKC pathway, leading to the inhibition of *Hydroides* metamorphosis in response to Mif1. In a screen of 300 kinases, Ro 32–0432 and Bis IV inhibited 9 and 4 non-PKC kinases by more than 80%, respectively (Anastassiadis et al., 2011). In addition to PKCs, Bis IV also inhibits Protein Kinase A at a higher concentration (IC50 of 11.8 μ M) (Davis et al., 1992). Both Ro 32–0432 and Bis IV strongly inhibit Ribosomal protein S6 Kinase alpha-2 (RSK3) and Ro 32–0432 also inhibits other genes in the RSK family, likely because the N-terminal kinase domain is part of the AGC family of kinases, which include PKC's kinase domain (Anastassiadis et al., 2011). RSK kinases are downstream of ERK1/2 and p38 (Anjum and Blenis, 2008), and because

ERK1/2 and p38 MAPKs are implicated in Hydroides metamorphosis (Shikuma et al., 2016), it is plausible that Ro 32-0432 and/or Bis IV inhibits metamorphosis through RSK. Other kinases that are inhibited by both Bis IV and Ro 32-0432 are the Glycogen Synthase Kinase-3 (GSK-3) α and β isoforms (Anastassiadis et al., 2011). GSK-3 is known to modulate diverse processes including growth, differentiation and apoptosis in human cells (Patel and Woodgett, 2017). These processes are all critical for metamorphosis, although it is unknown whether and/or how inhibition of GSK-3 could block metamorphosis in Hydroides. In humans the inhibitor Ro 32–0432 and Bis VIII (the same class of compounds as Bis IV) have been shown to promote the phosphorylation of p38 and JNK MAPK proteins (Kamiguti et al., 2003; Ohtsuka and Zhou, 2002) and commercial phospho-antibodies to p38 and JNK MAPK cross-react with Hydroides homologs (Shikuma et al., 2016). When Hydroides larvae were exposed to Bis IV we observed that p38 and JNK total protein and protein phosphorylation increased (Fig. S1A), while exposure to Ro 32-0432 marginally increased p38 phosphorylation (Fig. S1B). These results are consistent with the effects of Ro 32-0432 and Bis VIII on p38 and JNK MAPK phosphorylation responses in human cell lines.

Our observation that PKC inhibitors block Hydroides metamorphosis are consistent with other studies implicating PKC in the metamorphosis of other marine invertebrates. Larvae of the Annelid, Capitella sp. 1, undergo metamorphosis in response to arachidonic acid and the known morphogen, juvenile hormone (JH), a hormone which stimulates the PKC pathway in insects (Biggers and Laufer, 1996, 1999; Liu et al., 2015). Additionally, diacylglycerol promotes the metamorphosis of the Cnidarian, Hydractinia echinata, and metamorphosis is inhibited by a kinase inhibitor, staurosporine, which inactivates the PKC pathway (Leitz and Klingmann, 1990). In the Cnidarian, Cassiopea andromeda, Thieme et al. use the inhibitor Ro 32-0432 to implicate PKC in head morphogenesis from larvae-like buds (Thieme and Hofmann, 2003). Metamorphosis in insects, which are not known to require an external cue to undergo metamorphosis, also utilize PKC signaling in regulating metamorphosis. The mosquito Aedes aegypti utilizes the metamorphosis regulating chemical juvenile hormone-III to stimulate PKC via the phospholipase C pathway (Liu et al., 2015). With the addition of the data presented here, we can hypothesize that PKC has been adapted by Hydroides as a signaling pathway used to respond to bacteria and stimulate metamorphosis.

MACs stimulate the expression and localization of two nuclear hormone receptor genes. Nuclear hormone receptors play key roles in regulating gene expression in response to hormonal signals during metamorphosis in insects and amphibians, and PKC has been shown

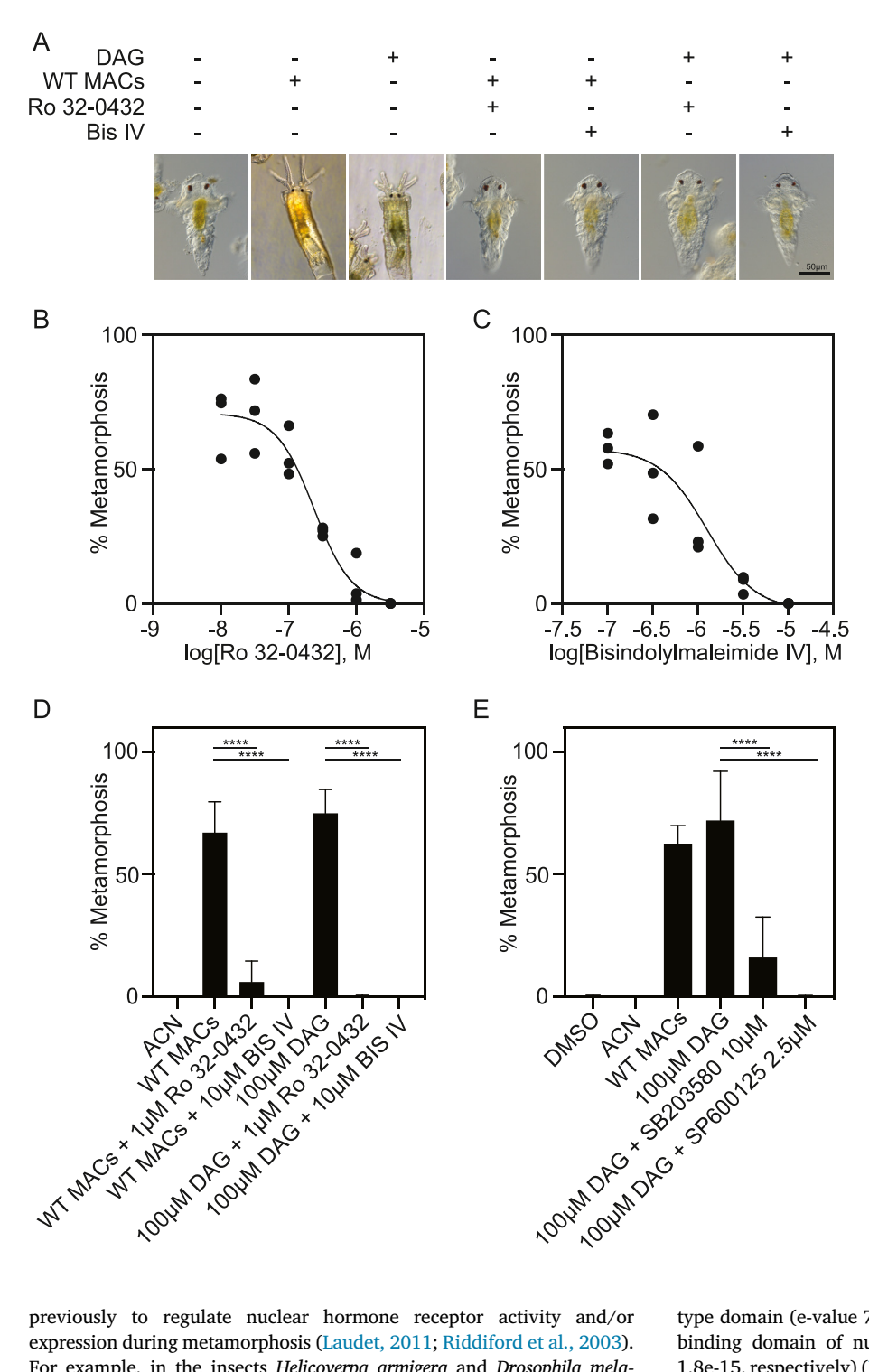


Fig. 3. Hydroides requires PKC and MAPK signaling to undergo metamorphosis in response to Mif1 and DAG. (A) Treatment combinations and representative images of larvae after 24 h of treatment with each condition, the IC50 was used for inhibitors and 100 µM DAG was used to strongly stimulate metamorphosis. (B and C) Hydroides metamorphosis in response to MACs, with a 1-h pre-treatment of increasing concentrations of the PKC inhibitors Ro 32-0432 IC50 = 235 nM (B), or bisindolylmaleimide IV (Bis IV) IC50 = $1.259 \mu M$ (C). Data points indicate individual biological replicates (n = 3). Each biological replicate plotted is the average of 4 technical replicates, where larvae from each replicate were derived from different male and female individuals. (D) Metamorphosis assay with wild type MACs or 1.2dioctanoyl-sn-glycerol (DAG) as the larvae inducer and 1-h pre-treatment with PKC inhibitors. (E) Metamorphosis assay with MAPK inhibitors in the presence of 1,2-dioctanoyl-sn-glycerol. Data are presented as mean of 3 biological replicates, where larvae from each replicate were derived from different male and female individuals, with error bars indicating standard deviation. Significance was determined by a one-way ANOVA with Tukey's multiple comparisons test. Comparisons are indicated by the line above compared conditions and **** represents p-values <0.0001.

previously to regulate nuclear hormone receptor activity and/or expression during metamorphosis (Laudet, 2011; Riddiford et al., 2003). For example, in the insects *Helicoverpa armigera* and *Drosophila melanogaster*, PKC phosphorylates the ecdysone receptor (EcR), modulating EcR activity during metamorphosis (Chen et al., 2017; Sun et al., 2007). Additionally, EcR expression has been shown to be localized to the brain during silk moth metamorphosis (Hossain et al., 2006). We therefore hypothesized that *Hydroides* possesses one or more nuclear hormone receptors that are regulated by PKC in the larval brain, and that Ro 32–0432 and Bis IV would inhibit this regulation.

We identified two putative nuclear hormone receptors in *Hydroides* located on different genomic contigs (hereafter, HeNHR1 and HeNHR2) that were upregulated 4.09 fold and 4.15 fold 30-min after bacteriastimulated metamorphosis, respectively (Table 1) (Shikuma et al., 2016). Both HeNHR1 and HeNHR2 contain the putative Zinc finger C4

type domain (e-value 7.5e-26 and 7.5e-26, respectively) and the ligand binding domain of nuclear hormone receptors (e-value 1.8e-15 and 1.8e-15, respectively) (Fig. 4A), and both domains together are indicative of nuclear hormone receptor transcription factors.

To observe the expression and localization of HeNHR1 and HeNHR2 transcripts within *Hydroides* larvae with or without MACs and PKC inhibitors Ro 32–0432 and Bis IV, we performed Whole Mount *In Situ* Hybridization (WMISH). To this end, seven-day old larvae were treated for 1 h with 1 μ M Ro 32–0432, 10 μ M Bis IV or DMSO solvent control and then subjected to WT MACs or buffer for 1 h prior to fixation. WMISH using HeNHR1 and HeNHR2-specific probes were stained for an equivalent time between compared groups (Buffer, MACs, MACs with Ro 32–0432, and MACs with Bisindolylmaleimide IV). In larvae treated with MACs, HeNHR1 and HeNHR2 staining occurred in the larval cerebral ganglia (Figs. 4C, 4G, S2C and S2D), while buffer-treated larvae did not

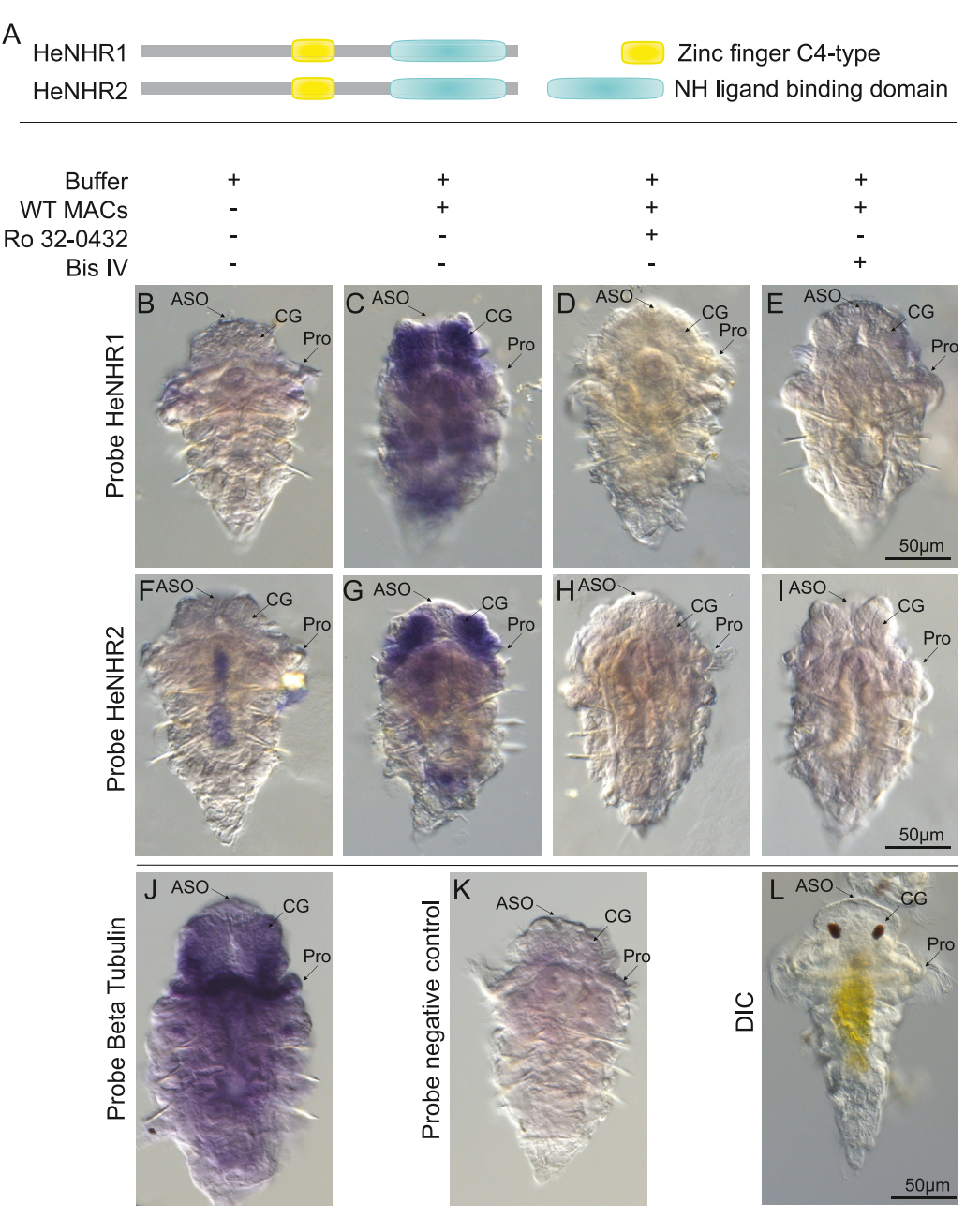


Fig. 4. Mif1 induces HeNHR1 and HeNHR2 expression through PKC signaling. (A) Domain architecture of Hydroides Nuclear Hormone Receptors, HeNHR1 and HeNHR2 (B-K) Competent larvae were pretreated for 1 h with 1 µM Ro 32-0432 or 10 µM bisindolylmaleimide IV or solvent, and then subsequently exposed to WT MACs to induce metamorphosis for an additional hour. The larvae were then probed with Digoxigenin-11-UTP labeled RNA for nuclear hormone receptors HeNHR1 (B-E) and HeNHR2 (F-I), beta tubulin (J) or a negative control (K) and visualized by NBT/BCIP staining. Anatomical structures indicated, (ASO) apical sensory organ, (CG) cerebral ganglia, and (Pro) prototroch. An image of a live larva is shown for reference (L). Representative images are shown from three biological replicates (See Fig. S2 for representative images from each biological replicate).

show localization or high expression of either nuclear hormone receptor in the same anatomical location (Figs. 4B, 4F, S2A and S2B). When the larvae were treated with either Ro 32–0432 or Bis IV before subjection to MACs, the larvae did not show localization or upregulation of HeNHR1 and HeNHR2 to the cerebral ganglia (Fig. 4D, E, 4H, 4I, and S2E-H). Our results show that *Hydroides* upregulates two nuclear hormone receptors in the cerebral ganglia during metamorphosis, resembling the regulation of EcR during insect metamorphosis. Further, our results show that Ro 32–0432 and Bis IV inhibitors block HeNHR1 and HeNHR2 localization or upregulation. The full characterization of HeNHR1 and HeNHR2 and their role of in *Hydroides* metamorphosis will be the subject of a future work.

PKC has been proposed previously to act as a node in a multi-step signal transduction process during bacteria-stimulated metamorphosis in the hydrozoan *Phialidium gregarium* (McCauley, 1997). In the proposed model, serotonin (5-HT) is released by producing cells, which binds nearby cells causing membrane depolarization and Ca2+ influx, activating PKC signaling and subsequent metamorphic events. The proposed

model of 5-HT action was suggested to be different in *Hydroides* (Nedved, 2010), in part, because the known PKC activator, 12-O-Tetradecanoyl-phorbol-13-Acetate (TPA), a phorbol ester, was insufficient to stimulate *Hydroides* metamorphosis (Holm et al., 1998). It is unclear why 1,2-dio-ctanoyl-sn-glycerol stimulates metamorphosis in *Hydroides* (Fig. 1D), while TPA does not. However, it has been proposed that the activation of PKC by DAG and TPA is not equivalent (Slater et al., 1996), and the pathways stimulated by TPA in *Hydroides* might differ from those of activated by DAG, as seen by our data. Our observation that HeNHR1/2 are expressed in the larval cerebral ganglia is consistent with a model where 5-HT positive cells activate PKC and HeNHR1/2 expression during *Hydroides* metamorphosis.

MACs and Mif1 activate *Hydroides* metamorphosis through DAG production, PKC and MAPK. We previously reported that the p38 and JNK MAPKs are required for the stimulation of *Hydroides* metamorphosis by MACs (Shikuma et al., 2016). To further define the signaling pathway involving DAG during the metamorphosis of *Hydroides*, we pre-exposed larvae to the p38 inhibitor SB203580 or the JNK inhibitor SP600125,

at the same effective concentrations established previously, $10~\mu M$ and $2.5~\mu M$, respectively (Shikuma et al., 2016), and stimulated metamorphosis using DAG (Fig. 3D). We found that DAG is unable to stimulate metamorphosis when larvae are exposed to either SB203580 or SP600125 MAPK inhibitors. These data suggest that MAPK signaling is downstream of DAG signaling during $\mbox{\it Hydroides}$ metamorphosis and suggest that both the PKC and MAPK pathways are required for metamorphosis.

There are discernible parallels between bacteria-stimulated metamorphosis in Hydroides and other PKC-, MAPK- and nuclear hormone receptor-mediated host-microbe interactions in other model organisms. For example, PKC delta and p38 MAPK were shown previously to regulate innate immunity in the roundworm Caenorhabditis elegans, by mediating the production of antimicrobial peptides in response to a fungal pathogen (Ziegler et al., 2009). These innate immune responses allowed for non-redundant signaling of another PKC isozyme and release of an antimicrobial peptide. PKC control of the MAPK pathway has very dramatic implications for the response of the cell to a given stimulus from simple heat shock response in Saccharomyces cerevisiae, and to the control of mechanosensory response in C. elegans (Hyde et al., 2011; Kamada et al., 1995). In C. elegans, the nuclear hormone receptor NHR-86 and p38 MAPK drive immune effector gene expression that provide protection against Pseudomonas aeruginosa (Peterson et al., 2019). In Drosophila, juvenile hormone and the ecdysone receptor (EcR), which play key roles in metamorphosis, have also been shown to induce and potentiate antimicrobial peptide gene expression (Flatt et al., 2008). Our future work into the function(s) of Mif1 that stimulate metamorphosis may provide insight into how P. luteoviolacea stimulates DAG production, and PKC/MAPK/NHR signal transduction. Understanding the cell signaling pathways that are regulated by P. luteoviolacea and its Mif1 effector informs our growing understanding of how bacteria can promote development in eukaryotic organisms.

Conclusion. Diacylglycerol, PKC and MAPK are highly conserved signaling systems found in diverse metazoans. The present work defines a working model of how *P. luteoviolacea* stimulates *Hydroides* metamorphosis. In this model pathway, MACs and Mif1 produced by bacteria stimulate an increase in DAG. DAG then signals the downstream pathways of PKC and MAPK signaling and activates the expression of two nuclear hormone receptors, HeNHR1 and HeNHR2 to promote metamorphosis. Defining these cascades are important for understanding bacteria-stimulated metamorphosis in *Hydroides* and provides a step toward our broader understanding of how bacteria promote animal development. Defining the signaling systems responsible for metamorphosis in *Hydroides* provides insight that may inform efforts to promote ecosystem remediation or antifouling technologies.

3. Materials and methods

Hydroides **Collection and Maintenance.** Specimens of *Hydroides elegans* were collected from Quivira Basin, San Diego, CA and propagated as described previously (Shikuma et al., 2014). Briefly, gametes were harvested from adult animals. Fertilized embryos were mixed and moved to a 1 L beaker containing 0.45 μ m filtered artificial seawater with *Isochrysis* algae (6 \times 10⁴ cells/mL). On the second day, larvae were diluted to 5 larvae/mL. Water changes were performed, and new algae was added daily until reaching competence (6–8 days).

Production of MACs Extract. Purification of MACs was carried out as previously described (Rocchi et al., 2019). Briefly, from frozen stock, *Pseudoalteromonas luteoviolacea* HI1 and genetic derivatives were struck out to single colonies on to Sea Water Tryptone (SWT) media (35.9 g/L Instant Ocean, 2.5 g/L tryptone, 1.5 g/L yeast extract, 1.5 mL/L glycerol, 15 g/L agar for solid media) and grown overnight at 30 °C. A single colony was inoculated into 5 mL SWT culture and grown overnight at 30 °C, 200 rpm. The overnight culture was inoculated at 1:100 into a 50 mL flask and grown for 10 h at 30 °C, 200 rpm. The 50 mL overnight culture was then centrifuged at 4,800 rcf for 20 min at 4 °C. The supernatant was

removed, and the pellet was gently suspended in 5 mL of extraction buffer (20 mM Tris Base, 1 M NaCl, pH 7.5) with aid of a serological pipette. The suspended pellet was then centrifuged again at 4,800 rcf for 20 min at 4 $^{\circ}$ C. The supernatant was then removed and again centrifuged at 4,800 rcf for 20 min at 4 $^{\circ}$ C to remove any remaining cells. After centrifugation only the top 3 mL of supernatant was removed. MAC extract up to 2 days old was used for metamorphosis assays.

Metamorphic induction of larvae and extraction of total lipids. Larvae were grown for 7 days until reaching competency, as described above. Larvae were then exposed to extraction buffer (20 mM Tris, 1M NaCl, pH 7.5), or extracted MACs from P. luteoviolacea wild type, $\Delta macB$ or $\Delta mif1$. The larvae were incubated with the MACs or buffer control at a 1:50 concentration for 1 h. After incubation, larvae were then subjected to lipid extraction following the previously established Bligh Dyer protocol (Bligh and Dyer, 1959). In brief, ASW was removed and the larvae were resuspended in 300 µL of 1:2 mixture of chloroform:methanol and vortexed vigorously for 2 min. An additional 100 µL of chloroform was added and the sample vortexed for another 30 sec. $100 \, \mu L$ of water was then added to separate the organic and aqueous layers and briefly vortexed. The sample was then centrifuged at >10,000 G for 10 min to further clarify the layers. The aqueous phase was then subject to UV 280 nm protein concentration analysis to determine relative quantities of larval protein extract and to normalize the total lipid concentrations. The chloroform phase was removed and dried under nitrogen stream. Samples were resuspended with 100% acetonitrile normalized by protein concentration to a total concentration of 4.94 mg/mL. The sample was resuspended via repeated water bath sonication for 5 min and vortexing for 30 s totaling 5 times.

Metabolomics analyses of Hydroides larvae exposed to MACs. Untargeted LCMS analyses were performed on the tubeworm extracts using a Bruker Elute UHPLC coupled with an Impact II QTOF mass spectrometer. The first analysis was performed on a 2 mm Dacapo DX-C18 column (Imtakt, Portland OR, USA) in reverse phase. A gradient elution was used from 40% channel A (0.1% formic acid in 98% water and 2% acetonitrile) to 100% channel B (0.1% formic acid in 98% acetonitrile and 2% water) over 22 min with a hold of 100% channel B over 10 min using a flow rate of 200 μ L/min and a 5 μ L injection volume. The mass spectrometer was operated in positive mode using a mass range of 50–1000 m/z at a scan rate of 8 Hz. The end plate offset was set to 500V, the capillary voltage was set to 4200 V with nebulizer gas pressure set at 1.0 bar, the dry gas flow rate at 5.0 L/min and the dry gas temperature at 250 $^{\circ}$ C. Ion funnels 1 and 2 were set to 200 and 400 V respectively. The hexapole was set to 90 V. The quadrupole ion energy was set to 3.0 eV and low mass set to 50 m/z. The collision cell collision energy was set to 7 eV, and a pre-pulse storage time of 7.5 μs. Stepping was used with the mode on basic, the always collision RF went from 900.0 to 2500.0 V with a transfer time from 27.0 to 90.0 μ s and timing from 10 to 90%. The MS/MS only collision energy went from 50 to 125% and the timing went from 50 to 50%. The Scan mode was on MRM with the number of precursors as 5. The threshold absolute threshold (per 1000 sum.) was 31 cts. Smart Exclusion with 5x. Active exclusion excluded after 3 Spectra, released after 1.00 min, with a Reconsidered Precursor, if the current intensity/previous intensity is at 5.0. Untargeted data was analyzed using XCMS Online (Gowda et al., 2014), using a multigroup job to identify lipid metabolites significantly different (p < 0.01, fold change >0.05) between larvae extracts exposed to buffer, MACs extracted from *P. luteoviolacea*, wild type, $\Delta macB$ and $\Delta mif1$. The data are publicly available at XCMS (https://xcmsonline.scripps.edu/la nding_page.php?pgcontent=listPublicShares) public job id #1502723.

Identification of PKC homologs in the *Hydroides* genome. Seven *Hydroides* PKC genes and gene homologs were found by BLASTn using the ten known human PKC isoforms as queries against the translated genome of *Hydroides elegans* (Shikuma et al., 2016). Once identified, the selected genes and isoforms of those genes were then searched against the NCBI non-redundant database using a PSI-BLAST and performing 5 iterations with a E-value cutoff of 0.05 and 500 sequences per iteration (Schäffer

et al., 2001). PKC proteins were searched for known domains by HMMER biosequence analysis using hidden Markov models (Finn et al., 2011), where significant hits to Pfam or Gene3d were identified (Table S2). A maximum likelihood phylogeny was generated using the human PKC isoforms and the seven identified Hydroides PKC genes. An alignment was first performed using Mafft e-ins-i alignment with default parameters (Katoh and Standley, 2013). Aligned amino acid sequences were used to generate a maximum likelihood tree using PhyML through the ATGC Montpellier Bioinformatics Platform (Guindon and Gascuel, 2003). The Smart Model Selection (Guindon et al., 2010; Lefort et al., 2017) option was used to calculate the best substitution model for the data, in which LG + G + I + F was selected. The branches are supported by 100 resamples. A previously published transcriptome of Hydroides (Shikuma et al., 2016) was mined to identify expression levels of larval transcripts at 6 d and at 30 min post exposure to MACs (Table 1).

Hydroides metamorphosis assays. Competent Hydroides larvae were concentrated to 40 larvae/mL and incubated for 1 h with penicillin and streptomycin. The larvae and antibiotics were then transferred into 24well plates at 1 mL per well for a final concentration of ~40 larvae/ well. Inhibitors and activators used in this work include Ro 32-0432 hydrochloride, Tocris Bioscience, Cat# 1587. 1,2-Dioctanoyl-sn-glycerol, Cayman Chemical, Cat# 62225. Bisindolylmaleimide IV, Cayman Chemical, Cat # 13299. SB 203580 hydrochloride, Tocris Bioscience, Cat# 1402. SP 600125, Sigma-Aldrich, Cat# w5567. Inhibitors were dissolved in acetonitrile, or DMSO according to manufacturer recommendation. All assays included the appropriate solvent controls for the given inhibitor tested, solvent volume was equal across all inhibitor concentrations and control wells. Inhibitors were added 1 h prior to addition of either MACs or candidate inducers. The range of the concentration tested was determined by larval sensitivity and toxicity, ranging from 100 nM to 100 µM. Larval metamorphosis was scored visually 24 h after addition of MACs extracts or DAG. Metamorphosis was scored as positive for larvae observed to possess an elongated body, loss of cilia, formation of branchial rudiments and the formation of a calcareous tube. Assays were performed with at least 3 biological replicates (n = 3), where larvae were derived from different male and female individuals.

Pretreatment of larvae for Western blot and whole mount in situ hybridization. Larvae were first grown for 7 days following the collection and maintenance protocols. 1,000 larvae were then separated and concentrated into 2 mL of artificial sea water. Larvae were then treated with penicillin 100 $\mu g/mL$ and streptomycin 100 $\mu g/mL$ for 1 h. Inhibitors Ro-32-0432 1 μM and Bis IV 10 μM and solvent controls (ACN/DMSO) were then added to the larvae for another hour. MACs 1:75 dilution or 1,2-dioctanoyl-sn-glycerol was added to the larvae for a final hour before takedown.

Whole mount in situ hybridization. The WMISH procedure was modified from methods by Seaver and Kaneshige (2006). Sequences for HeNHR1 and HeNHR2 (Table S4) were identified from a previously performed Hydroides elegans transcriptome analysis (Shikuma et al., 2016). WMISH RNA probes were generated using the protocol outlined in (Hua et al., 2018). In short, total RNA was isolated from treated larvae via TRIzol (Thermo fisher CAT#15596018) and cDNA was created using oligo d(T)23VN primers (New England Biolabs CAT#E6300s). From the cDNA the 1st PCR product was produced and validated for size (Table S5). A second PCR with T7 RNA polymerase engineered reverse primers were used to make the template for the probes and were validated by sanger sequencing (Table S5). Probes were made using T7 RNA polymerase (Lucigen CAT#30223-1) with dioxigenin-UTP (Sigma Aldrich CAT#11209256910). The negative control probe was made using ascidian cDNA for a gene which is not present on the Hydroides genome. WMISH was performed by first relaxing larvae by adding 1 volume of 6.5% MgCl for 2 min. The larvae were fixed in 4% paraformaldehyde in 0.5M NaCl, 0.1M MOPS pH 7.5 overnight at 4 °C. The larvae were then dehydrated by washing in 25% EtOH in 1xPBS tween

(1.86 mM NaH₂PO₄ 8.41 mM Na₂HPO₄ 175 mM NaCl pH 7.4 0.1% tween-20), 50% EtOH PBS tween, and 75% EtOH PBS tween before storing them in 100% EtOH at -80 °C. The larvae were rehydrated by subsequent washes in 75%, 50%, 25%, 0% EtOH in PBS tween. Larvae were then digested with proteinase K 0.01 mg/mL in PBS tween for 5 min. The reaction was stopped with 3 washes in PBS tween plus 2 mg/mL glycine. The larvae were then washed in 1% triethanolamine with 1.5 μL/500 μL acetic anhydride twice. Then washed twice in PBS tween. The larvae were then refixed in 4% paraformaldehyde in PBS tween for 1 h at room temperature followed by five washes in PBS tween. To kill endogenous alkaline phosphatase the larvae were heated to 80 °C for 10 min in PBS tween. The larvae were then washed in hybridization buffer (50% formamide, 0.075 Na citrate, 750 mM NaCl, 50 $\mu g/mL$ heparin sodium (Selleck chemicals CAT#70288-86-7), 0.1% tween, 1% SDS, 50μg/mL herring sperm DNA, pH 4.5), and after the first wash was left in the hybridization buffer overnight at 60 $^{\circ}$ C. The probes were diluted to $3.0~\text{ng/}\mu\text{L}$ in hybridization buffer and boiled at 80 $^{\circ}\text{C}$ before being added to the larvae where they were allowed to hybridize for at least 48 h at 60 °C. The probe was removed, and the larvae were washed with 75% hybridization buffer and 25% 2X SSC (20x SSC 0.3M Na citrate and 3M NaCl). Followed by 50% hybridization buffer and 50% 2X SSC, then 25% hybridization buffer and 75% 2X SSC, finally by two washes with 2x SSC buffer. The larvae were then exchanged into PBS tween by washing with 0.05X SSC twice followed by, 75% 0.05X SSC and 25% PBS tween, then, 50% 0.05X SSC and 50% PBS tween, 25% 0.05X SSC and 75% PBS tween, finally by washing with 100% PBS tween five more times. The larvae were then blocked in 0.5% Roche blocking solution (Sigma Aldrich CAT#9000-7-1-9) in 0.1M Tris pH 7.5, 0.15M NaCl for 1 h. The blocking solution was washed and then the anti-DIG antibody (Sigma CAT# 11093274910) was added to the blocking buffer at 1:5000 dilution and the larvae were incubated at 4 °C overnight. The larvae were then washed 5 times in PBT (1xPBS, 0.2% Triton x-100 and 0.1% BSA, Thermo fisher CAT# AAJ6465522). The larvae were then washed in the alkaline phosphatase reaction buffer without MgCl, AP buffer (100 mM NaCl, 50 mM MgCl, 100 mM Tris pH 9.5, 0.5% tween-20). Then washed twice with the AP buffer to equilibrate the pH and prevent precipitation. The larvae were developed in AP buffer plus 200 μ L/10 mL NBT/BCIP stock solution (Millapore sigma CAT# 11681451001) in the dark until purple staining appeared (1hr for Beta tubulin prove, 2 h for HeNHR1, HeNHR2 and scramble probe). NBT/BCIP incubation was performed for the same amount of time for treatments exposed to each HeNHR1 or HeNHR2 probe. Larvae were then washed 5 times in PBS tween before mounting on slides in 80% glycerol.

Western blot. Protein was recovered on ice by first centrifuging larvae at 4000rpm for 5min and removing ~1950 µL of sea water and resuspending by vortexing larvae in a lysis solution of 50 mM tris pH 7.6, 1% Triton X-100, 150 mM NaCl. Larvae were then frozen at $-80\,^{\circ}$ C to aid in lysis. After thawing, the sample was centrifuged at 21,000g for 20min and the pellet was discarded. Protein was quantified by Bio-Rad protein assay (CAT #5000001). 15 µg of protein was loaded onto a 4-12% SDSpolyacrylamide gel and run for 60 min at 110V. The protein was then transferred onto a PVDF membrane. The membrane was dried and recharged with methanol. Membrane was washed with TBS tween 1% (TBST), 3 times and primary antibodies were added at a 1:1000 dilution and rocked in a 10% BSA TBST solution overnight (Cell Signaling Technologies CAT #s 9212, 9252, 9912, 9913). Membrane was washed 3x with TBST for $10\ min\ each$ and incubated with secondary-HRP (Novus Biological CAT#BP1-75306) conjugated antibody at 1:10,000 for 1 h 3x final washes with TBST for 15 min were performed before final visualization with West Femto substrate (Thermo Fisher CAT#34095) on a Bio-Rad Gel Doc XR.

Declaration of competing interest

The authors declare no competing interests.

Acknowledgements

We would like to thank Dr. Giselle Cavalcanti, Dr. Tiffany Dunbar, and Mr. Andriy Fedoriouk for their valuable feedback on the manuscript. This work was supported in part by the National Science Foundation (1942251, N.J.S.; 2017232404, A.T.A.), the Office of Naval Research (N00014-17-1-2677 and N00014-20-1-2120 N.J.S.), the Gordon and Betty Moore Foundation (GBMF9344, https://doi.org/10.37807/GBMF9344), the Alfred P. Sloan Foundation, Sloan Research Fellowship (N.J.S.) and the ARCS Foundation (K.E.M., A.T.A.).

Appendix A. Supplementary data

Supplementary data to this article can be found online at https://doi.org/10.1016/j.ydbio.2022.04.009.

References

- Amador-Cano, G., Carpizo-Ituarte, E., Cristino-Jorge, D., 2006. Role of protein kinase C, G-protein coupled receptors, and calcium flux during metamorphosis of the sea urchin Strongylocentrotus purpuratus. Biol. Bull. 210, 121–131. https://doi.org/ 10.2307/4134601
- Anastassiadis, T., Deacon, S.W., Devarajan, K., Ma, H., Peterson, J.R., 2011.
 Comprehensive assay of kinase catalytic activity reveals features of kinase inhibitor selectivity. Nat. Biotechnol. 29, 1039–1045. https://doi.org/10.1038/nbt.2017.
- Anjum, R., Blenis, J., 2008. The RSK family of kinases: emerging roles in cellular signalling. Nat. Rev. Mol. Cell Biol. 9, 747–758. https://doi.org/10.1038/nrm2509.
- Biggers, W.J., Laufer, H., 1999. Settlement and metamorphosis of Capitella larvae induced by juvenile hormone-active compounds is mediated by protein kinase C and ion channels. Biol. Bull. 196, 187–198. https://doi.org/10.2307/1542564.
- Biggers, W.J., Laufer, H., 1996. Detection of juvenile hormone-active compounds by larvae of the marine annelid *Capitella* sp. I. Arch. Insect Biochem. Physiol. 32, 475–484. https://doi.org/10.1002/(sici)1520-6327(1996)32:3/4<475::aid-arch19>3.0.co;2-9.
- Black, A.R., Black, J.D., 2012. Protein kinase C signaling and cell cycle regulation. Front. Immunol. 3, 1–18. https://doi.org/10.3389/fimmu.2012.00423.
- Bligh, E.G., Dyer, W.J., 1959. A rapid method of total lipid extraction and purification. Can. J. Biochem. Physiol. 37, 911–917. https://doi.org/10.1139/o59-099.
- Brose, N., Rosenmund, C., 2002. Move over protein kinase C, you've got company: alternative cellular effectors of diacylglycerol and phorbol esters. J. Cell Sci. 115, 4399–4411. https://doi.org/10.1242/jcs.00122.
- Brown, D.D., Cai, L., 2007. Amphibian metamorphosis. Dev. Biol. 306, 20-33.
- Bryan, P.J., Qian, P., Kreider, J.L., Chia, F., 1997. Induction of larval settlement and metamorphosis by pharmacological and conspecific associated compounds in the serpulid polychaete. Hydroides elegans. Mar Ecol Prog Ser 146, 81–90.
- Carpizo-ituarte, E., Hadfield, M.G., 2003. Transcription and translation inhibitors permit metamorphosis up to radiole formation in the serpulid polychaete *Hydroides elegans* haswell. Mar Biol Lab 204, 114–125. https://doi.org/10.2307/1543547.
- Carpizo-Ituarte, E., Hadfield, M.G., 1998. Stimulation of metamorphosis in the polychaete Hydroides elegans haswell (serpulidae). Biol. Bull. 194, 14–24.
- Cavalcanti, G., Alker, A., Delherbe, N., Malter, K.E., Shikuma, N.J., 2020. The influence of bacteria on animal metamorphosis. Annu. Rev. Microbiol. 74. https://doi.org/ 10.1146/annurev-micro-011320-012753 (in press).
- Chambon, J.P., Nakayama, A., Takamura, K., McDougall, A., Satoh, N., 2007. ERK- and JNK-signalling regulate gene networks that stimulate metamorphosis and apoptosis in tail tissue of ascidian tadpoles. Development 134, 1203–1219. https://doi.org/ 10.1242/dev.002220.
- Chen, C.H., Pan, J., Di, Y.Q., Liu, W., Hou, L., Wang, J.X., Zhao, X.F., 2017. Protein kinase C delta phosphorylates ecdysone receptor B1 to promote gene expression and apoptosis under 20-hydroxyecdysone regulation. Proc. Natl. Acad. Sci. U. S. A. 114, E7121–E7130. https://doi.org/10.1073/pnas.1704999114.
- Davis, P.D., Hill, C.H., Lawton, G., Nixon, J.S., Wilkinson, S.E., Hurst, S.A., Keech, E., Turner, S.E., 1992. Inhibitors of protein kinase C. 1. 2,3-Bisarylmaleimides. J. Med. Chem. 35, 177–184. https://doi.org/10.1021/jm00079a024.
- Ericson, C.F., Eisenstein, F., Medeiros, J.M., Malter, K.E., Cavalcanti, G.S., Zeller, R.W., Newman, D.K., Pilhofer, M., Shikuma, N.J., 2019. A contractile injection system stimulates tubeworm metamorphosis by translocating a proteinaceous effector. Elife 8, 1-19. https://doi.org/10.7554/eLife.46845.
- Fabre, S., Prudhomme, M., Rapp, M., 1993. Protein kinase C inhibitors; Structure—activity relationships in K252c-related compounds. Bioorg. Med. Chem. 1, 193–196. https://doi.org/10.1016/S0968-0896(00)82121-5.
- Finn, R.D., Clements, J., Eddy, S.R., 2011. HMMER web server: interactive sequence similarity searching. Nucleic Acids Res. 39, W29–W37. https://doi.org/10.1093/nar/ gkr367.
- Flatt, T., Heyland, A., Rus, F., Porpiglia, E., Yamamoto, R., Garbuzov, A., Palli, S.R., Tatar, M., Silverman, N., 2008. Hormonal regulation of the humoral innate immune response in Drosophila melanogaster. J. Exp. Biol. 211, 2712–2724. https://doi.org/ 10.1242/jeb.014878.
- Freeman, G., Ridgway, E.B., 1990. Cellular and intracellular pathways mediating the metamorphic stimulus in hydrozoan planulae. Roux's Arch. Dev. Biol. 199, 63–79. https://doi.org/10.1007/BF02029553.

- Gilbert, S.F., Bosch, T.C.G., Ledón-Rettig, C., 2015. Eco-Evo-Devo: developmental symbiosis and developmental plasticity as evolutionary agents. Nat. Rev. Genet. 16, 611–622. https://doi.org/10.1038/nrg3982.
- Gowda, H., Ivanisevic, J., Johnson, C.H., Kurczy, M.E., Benton, H.P., Rinehart, D., Nguyen, T., Ray, J., Kuehl, J., Arevalo, B., Westenskow, P.D., Wang, J., Arkin, A.P., Deutschbauer, A.M., Patti, G.J., Siuzdak, G., 2014. Interactive XCMS online: simplifying advanced metabolomic data processing and subsequent statistical analyses. Anal. Chem. 86, 6931–6939. https://doi.org/10.1021/ac500734c.
- Guindon, S., Dufayard, J., Lefort, V., Anisimova, M., Hordijk, W., Gascuel, O., 2010. New algorithms and methods to estimate maximim-likelihood phylogenies assessing the performance of PhyML 3.0. Syst. Biol. 59, 307–321.
- Guindon, S., Gascuel, O., 2003. A simple, fast, and accurate algorithm to estimate large phylogenies by maximum likelihood. Syst. Biol. 52, 696–704. https://doi.org/ 10.1080/10635150390235520.
- Hadfield, M.G., 2011. Biofilms and marine invertebrate larvae: what bacteria produce that larvae use to choose settlement sites. Ann. Rev. Mar. Sci 3, 453–470. https:// doi.org/10.1146/annurev-marine-120709-142753.
- Hadfield, M.G., 2000. Why and how marine-invertebrate larvae metamorphose so fast. Semin. Cell Dev. Biol. 11, 437–443. https://doi.org/10.1006/scdb.2000.0197.
- Hadfield, M.G., Carpizo-Ituarte, E.J., Carmen, K Del, Nedved, B.T., 2001. Metamorphic competence, a major adaptive convergence in marine invertebrate larvae. Am. Zool. 41, 1123–1131. https://doi.org/10.1093/icb/41.5.1123.
- Henningi, G., Hofmann, D.K., Yahu, Y.B., 1998. Metamorphic processes in the soft corals heteroxenia fiuscescens and xenia umbellata: the effect of protein kinase c activators and inhibitors. Invertebr. Reprod. Dev. 34, 35–45. https://doi.org/10.1080/ 07924259.1998.9652351.
- Hill, R.J., Billas, I.M.L., Bonneton, F., Graham, L.D., Lawrence, M.C., 2013. Ecdysone receptors: from the ashburner model to structural biology. Annu. Rev. Entomol. 58, 251–271. https://doi.org/10.1146/annurev-ento-120811-153610.
- Holm, E.R., Nedved, B.T., Carpizo-Ituarte, E., Hadfield, M.G., 1998. Metamorphic-signal transduction in Hydroides elegans (polychaeta: serpulidae) is not mediated by a G protein. Biol. Bull. 195, 21–29. https://doi.org/10.2307/1542772.
- Hossain, M., Shimizu, S., Fujiwara, H., Sakurai, S., Iwami, M., 2006. EcR expression in the prothoracicotropic hormone-producing neurosecretory cells of the *Bombyx mori* brain: an indication of the master cells of insect metamorphosis. FEBS J. https://doi.org/10.1111/j.1742-4658.2006.05398.x.
- Hua, R., Yu, S., Liu, M., Li, H., 2018. A PCR-based method for RNA probes and applications in neuroscience. Front. Neurosci. 12, 1–11. https://doi.org/10.3389/ fnins.2018.00266.
- Huang, S.Y., Hadfield, M.G., 2003. Composition and density of bacterial biofilms determine larval settlement of the polychaete Hydroides elegans. Mar Ecol Ser 260, 161–172.
- Huang, Y., Callahan, S., Hadfield, M.G., 2012. Recruitment in the Sea: Bacterial Genes Required for Inducing Larval Settlement in a Polychaete Worm. https://doi.org/ 10.1038/srep00228.
- Hyde, R., Corkins, M.E., Somers, G.A., Hart, A.C., 2011. PKC-1 acts with the ERK MAPK signaling pathway to regulate *C. elegans* mechanosensory response. Gene Brain Behav. 10, 286–298. https://doi.org/10.1038/jid.2014.371.
- Kamada, Y., Jung, U.S., Piotrowski, J., Levin, D.E., 1995. The protein kinase C-activated MAP kinase pathway of Saccharomyces cerevisiae mediates a novel aspect of the heat shock response. Genes Dev. 9, 1559–1571.
- Kamiguti, A.S., Harris, R.J., Slupsky, J.R., Baker, P.K., Cawley, J.C., Zuzel, M., 2003. Regulation of hairy-cell survival through constitutive activation of mitogen-activated protein kinase pathways. Oncogene 22, 2272–2284. https://doi.org/10.1038/ sj.onc.1206398.
- Katoh, K., Standley, D.M., 2013. MAFFT multiple sequence alignment software version 7: improvements in performance and usability. Mol. Biol. Evol. 30, 772–780. https://doi.org/10.1093/MOLBEV/MST010.
- Laudet, V., 2011. The origins and evolution of vertebrate metamorphosis. Curr. Biol. 21, R726–R737. https://doi.org/10.1016/j.cub.2011.07.030.
- Lawrence, I.G., Jamshed, R.T., Burr, G.A., 1996. Metamorphosis Postembryonic Reprogramming of Gene Expression in Amphibian and Insect Cells. Academic press. https://doi.org/10.1016/B978-0-12-283245-1.50023-3.
- Lefort, V., Longueville, J.-E., Gascuel, O., 2017. SMS: smart model selection in PhyML. Mol. Biol. Evol. 34, 2422–2424. https://doi.org/10.1093/MOLBEV/MSX149.
- Leise, E.M., Thavaradhara, K., Durham, N.R., Turner, B.E., 2001. Serotonin and nitric oxide regulate metamorphosis in the marine snail. Ilyanassa obsoleta. Am Zool 41, 258–267.
- Leitz, T., Klingmann, G., 1990. Metamorphosis in *Hydractinia*: studies with activators and inhibitors aiming at protein kinase C and potassium channels. Roux's Arch. Dev. Biol. 199, 107–113. https://doi.org/10.1007/BF02029558.
- Leitz, T., Müller, W.A., 1987. Evidence for the involvement of PI-signaling and diacylglycerol second messengers in the initiation of metamorphosis in the hydroid Hydractinia echinata Fleming. Dev. Biol. 121, 82–89. https://doi.org/10.1016/0012-1606(87)90140-0.
- Leitz, T., Wagner, T., 1993. The marine bacterium Alteromonas espejiana induces metamorphosis of the hydroid Hydractinia echinata. Mar. Biol. 115, 173–178. https://doi.org/10.1007/BF00346332.
- Li, Z., 2011. The Relationship of Protein Kinase C and Nitric Oxide Signaling in Metamorphosis of Marine Gastropod Larvae, *Crepidula Fornicata*. Dickinson College Hange Theore.
- Liang, X., Chen, Y.R., Gao, W., Guo, X.P., Ding, D.W., Yoshida, A., Osatomi, K., Yang, J.L., 2018. Effects on larval metamorphosis in the mussel *Mytilus coruscus* of compounds that act on downstream effectors of G-protein-coupled receptors. J. Mar. Biol. Assoc. U. K. 98, 333–339. https://doi.org/10.1017/S0025315416001417.

- Liu, P., Peng, H.-J., Zhu, J., 2015. Juvenile hormone-activated phospholipase C pathway enhances transcriptional activation by the methoprene-tolerant protein. Proc. Natl. Acad. Sci. Unit. States Am. 112, E1871–E1879. https://doi.org/10.1073/ pnas.1423204112.
- McCauley, D.W., 1997. Serotonin plays an early role in the metamorphosis of the hydrozoan *Phialidium gregarium*. Dev. Biol. 190, 229–240. https://doi.org/10.1006/ dbio.1997.8698
- Nedved, B.T., 2010. Neuromuscular Development and Metamorphosis in the Serpulid Polychaete Hydroides Elegans. UNIVERSITY OF HAWAI'I AT MANOĀ, Honolulu.
- Nedved, B.T., Hadfield, M.G., 2009. Hydroides elegans (Annelida: polychaeta): a model for biofouling Research. Mar idustrial biofouling 4, 203–217. https://doi.org/ 10.1007/978-3-540-69796-1_11.
- Nishizuka, Y., 1995. Protein kinase C and lipid signaling for sustained cellular responses. FASEB 9, 484–496. https://doi.org/10.1096/fasebj.9.7.7737456.
- Nishizuka, Y., 1992. Intracellular signaling by hydrolysis of phospholipids and activation of protein kinase C. Science 258 (80), 607–614. https://doi.org/10.1126/science 1411571
- Ohtsuka, T., Zhou, T., 2002. Bisindolylmaleimide VIII enhances DR5-mediated apoptosis through the MKK4/JNK/p38 kinase and the mitochondrial pathways. J. Biol. Chem. 277, 29294–29303. https://doi.org/10.1074/jbc.M203342200.
- Patel, P., Woodgett, J.R., 2017. Glycogen Synthase kinase 3: a kinase for all pathways? Curr. Top. Dev. Biol. 123, 277–302. https://doi.org/10.1016/BS.CTDB.2016.11.011.
- Pearce, C.M., Scheibling, R.E., 1994. Induction of metamorphosis of larval echinoids (Strongylocentrotus droebachiensis and Echinarachnius parma) by potassium chloride (KCI). Invertebr. Reprod. Dev. 26, 213–220. https://doi.org/10.1080/ 07924259 1994 9672420
- Peterson, N.D., Cheesman, H.K., Liu, P., Anderson, S.M., Foster, K.J., Chhaya, R., Perrat, P., Thekkiniath, J., Yang, Q., Haynes, C.M., Pukkila-Worley, R., 2019. The nuclear hormone receptor NHR-86 controls anti-pathogen responses in *C. elegans*. PLoS Genet. 15, 1–19. https://doi.org/10.1371/journal.pgen.1007935.
- Riddiford, L.M., Hiruma, K., Zhou, X., Nelson, C.A., 2003. Insights into the molecular basis of the hormonal control of molting and metamorphosis from *Manduca sexta* and *Drosophila melanogaster*. Insect Biochem. Mol. Biol. 33, 1327–1338. https://doi.org/ 10.1016/j.ibmb.2003.06.001.
- Rocchi, I., Ericson, C.F., Malter, K.E., Zargar, S., Eisenstein, F., Pilhofer, M., Beyhan, S., Shikuma, N.J., 2019. A bacterial phage tail-like structure kills eukaryotic cells by injecting a nuclease effector. Cell Rep. 28, 295–301. https://doi.org/10.1016/ i.celrep.2019.06.019 e4.
- Schäffer, A.A., Aravind, L., Madden, T.L., Shavirin, S., Spouge, J.L., Wolf, Y.I., Koonin, E.V., Altschul, S.F., 2001. Improving the accuracy of PSI-BLAST protein database searches with composition-based statistics and other refinements. Nucleic Acids Res. 29, 2994–3005. https://doi.org/10.1093/nar/29.14.2994.
- Schneider, T., Leitz, T., 1994. Protein kinase C in hydrozoans: involvement in metamorphosis of *Hydractinia* and in pattern formation of *Hydra*. Roux's Arch. Dev. Biol. 203, 422–428. https://doi.org/10.1007/BF00188691.
- Seaver, E.C., Kaneshige, L.M., 2006. Expression of "segmentation" genes during larval and juvenile development in the polychaetes *Capitella sp. I* and *H. elegans*. Dev. Biol. 289, 179–194. https://doi.org/10.1016/j.ydbio.2005.10.025.
- Shikuma, N.J., 2021. Bacteria-stimulated metamorphosis: an ocean of insights from investigating a transient host-microbe interaction. mSystems 6, 1–5. https://doi.org/ 10.1128/msystems.00754-21.

- Shikuma, N.J., Antoshechkin, I., Medeiros, J.M., Pilhofer, M., Newman, D.K., 2016. Stepwise metamorphosis of the tubeworm *Hydroides elegans* is mediated by a bacterial inducer and MAPK signaling. Proc. Natl. Acad. Sci. Unit. States Am. 113, 10097–10102. https://doi.org/10.1073/pnas.1603142113.
- Shikuma, N.J., Pilhofer, M., Weiss, G.L., Hadfield, M.G., Jensen, G.J., Newman, D.K., 2014. Marine tubeworm metamorphosis induced by arrays of bacterial phage tail-like structures. Science 343 (80), 529–533. https://doi.org/10.1126/science.1246794.
- Slater, S.J., Ho, C., Kelly, M.B., Larkin, J.D., Taddeo, F.J., Yeager, M.D., Stubbs, C.D., 1996. Protein kinase Cα contains two activator binding sites that bind phorbol esters and diacylglycerols with opposite affinities. J. Biol. Chem. 271, 4627–4631. https:// doi.org/10.1074/jbc.271.9.4627.
- Strader, M.E., Aglyamova, G.V., Matz, M.V., 2018. Molecular characterization of larval development from fertilization to metamorphosis in a reef-building coral. BMC Genom. 19, 1–17. https://doi.org/10.1186/s12864-017-4392-0.
- Sun, Y., An, S., Henrich, V.C., Sun, X., Song, Q., 2007. Proteomic identification of PKC-mediated expression of 20E-induced protein in drosophila melanogaster. J. Proteome Res. 6, 4478–4488. https://doi.org/10.1021/pr700709x.
- Tata, J.R., 1998. Hormonal Signaling and Postembryonic Development (Molecular Biology Intelligence Unit).
- Thieme, C., Hofmann, D.K., 2003. Control of head morphogenesis in an invertebrate asexually produced larva-like bud (Cassiopea andromeda; Cnidaria: scyphozoa). Dev. Gene. Evol. 213, 127–133. https://doi.org/10.1007/s00427-003-0300-5.
- Thiyagarajan, V., Wong, T., Qian, P.Y., 2009. 2D gel-based proteome and phosphoproteome analysis during larval metamorphosis in two major marine biofouling invertebrates. J. Proteome Res. 8, 2708–2719. https://doi.org/10.1021/ pr800976u.
- Titball, R.W., 1993. Bacterial phospholipases C. Microbiol. Rev. 57, 347–366. https://doi.org/10.1128/MMBR.57.2.347-366.1993.
- Wilkinson, S.E., Parker, P.J., Nixon, J.S., 1993. Isoenzyme specificity of bisindolylmaleimides, selective inhibitors of protein kinase C. Biochem. J. 294.
- Wong, Y.H., Arellano, S.M., Zhang, H., Ravasi, T., Qian, P.Y., 2010. Dependency on de novo protein synthesis and proteomic changes during metamorphosis of the marine bryozoan. Bugula neritina. Proteome Sci 8, 1–14. https://doi.org/10.1186/1477-5956-8-25.
- Wu-Zhang, A.X., Newton, A.C., 2013. Protein kinase C pharmacology: refining the toolbox. Biochem. J. 452, 195–209. https://doi.org/10.1042/bj20130220.
- Yamamoto, H., Tachibana, A., Matsumura, K., Fusetani, N., 1995. Protein kinase C (PKC) signal transduction system involved in larval metamorphosis of the barnacle. Balanus amphitrite. Zoolog Sci. https://doi.org/10.2108/zsj.12.391.
- Yool, A.J., Grau, S.M., Hadfield, M.G., Jensen, R.A., Markell, D.A., Morse, D.E., 1986. Excess potassium induces larval metamorphosis in four marine invertebrate species. Biol. Bull. 170, 255–266. https://doi.org/10.2307/1541807.
- Ziegler, K., Kurz, L.C., Cypowyj, S., Couillault, C., Pophillat, M., Pujol, N., Ewbank, J.J., 2009. Antifungal innate immunity in C. elegans: PKC d links G protein signaling and a conserved p38 MAPK cascade. Cell Host Microbe 5, 341–352. https://doi.org/ 10.1016/j.chom.2009.03.006.
- Zobell, C.E., Allen, E.C., 1934. The significance of marine bacteria in the fouling of submerged surfaces. J. Bacteriol. 29, 239–251.